Polymorphic Transformation of 1,3-Distearoyl-*sn*-2-linoleoyl-glycerol

M. Takeuchi[a,*], S. Ueno[a], J. Yano[a], E. Floter[b], and K. Sato[a]

[a]Faculty of Applied Biological Science, Hiroshima University, Higashi-Hiroshima, 739-8528, Japan, and

[b]Unilever Research Vlaardingen, 3133 AT Vlaardingen, The Netherlands

ABSTRACT: Polymorphic transformation behavior of sub-α_1, sub-α_2, α, and γ in 1,3-distearoyl-*sn*-2-linoleoyl-glycerol (SLS) has been studied with X-ray diffraction, differential scanning caloremetry, and Fourier-transform infrared spectroscopy. Synchrotron radiation X-ray beam was employed to observe rapid transformation processes from the sub-α and α forms to the γ form. The chain length structures were double in sub-α_1, sub-α_2, and α, whereas γ was of triple chain-length structure. The subcell packing was pseudohexagonal for the two sub-α forms, hexagonal for the α form, and parallel type for the γ form. In comparison with 1,3-distearoyl-*sn*-2-oleoyl-glycerol (SOS), the occurrence behavior of sub-α, α, and γ of SLS was the same as that of SOS. However, the absence of β' and β was unique for SLS. The chain–chain interactions between the linoleoyl moieties may stabilize the γ form, prohibiting the transformation into β' or β forms. The presence of two *cis* double bonds may cause this stabilization, revealing the disordered chain conformation of the unsaturated chains.

Paper no. J9553 in *JAOCS 77*, 1243–1249 (December 2000).

KEY WORDS: DSC, FTIR, linoleic acid, polymorphism, SLS (1,3-distearoyl-*sn*-2-linoleoyl-glycerol), synchrotron radiation X-ray diffraction.

Triacylglycerols (TAG) are major nutrients together with carbohydrates and proteins, and are widely employed as fats in foods and in the cosmetics and pharmaceuticals industries (1). Many TAG present in vegetable fats and oils contain saturated and unsaturated fatty acid moieties connected to a glycerol group (mixed-acid TAG). Polymorphic properties of saturated-unsaturated mixed-acid TAG (St. U. St. TAG) containing oleic acid have been examined including SOS (1,3-distearoyl-*sn*-2-oleoyl-glycerol), POP (1,3-dipalmitoyl-*sn*-2-oleoyl-glycerol) (2–4); POS (1-palmitoyl-2-oleoyl-3-stearoyl-glycerol) (5); BOB (1,3-dibehenoyl-*sn*-2-oleoyl-glycerol) (6); SSO (1,2-distearoyl-*sn*-3-oleoyl-glycerol) (7); and SRS (1,3-distearoyl-*sn*-2-ricinoleoyl-glycerol) (8).

The TAG containing linoleic acid moieties are also critically important, since linoleic acid is a polyunsaturated fatty acid having multiple nutritional functions (9). Physical and chemical properties of the St. U. St. TAG containing linoleic acid moiety are of high interest. In addition, genetically modified fats and oils involve higher amounts of linoleic and stearic acids. In particular, high-stearic acid seed oils reveal that the distribution of the fatty acids on the *sn*-2 position is highly dependent on the original crop selected for the high stearic variant. The distribution of the mono- and polyunsaturated fatty acids on the *sn*-2 position in the TAG containing one or two saturated fatty acids at the *sn*-1 and *sn*-3 positions strongly influences the properties of the St. U. St. TAG (10,11). In order to better understand what this implies for applications of TAG other than the well-studied cocoa butter component SOS, it is desirable to clarify the polymorphic behavior of SLS (1,3-distearoyl-*sn*-2-linoleoyl-glycerol).

The purpose of this work was to clarify the polymorphic properties of SLS. In the present work, four polymorphic forms, sub-α_2, sub-α_1, α, and γ, were isolated. However, no β' and β forms were detectable even after prolonged thermal treatment for stabilization. This indicates specific polymorphic properties for SLS, most probably due to chain–chain interactions between the linoleoyl and stearoyl moieties.

MATERIALS AND METHODS

Synthesis of SLS. TAG of this type are generally prepared according to the following scheme (12). In the first step, the sodium salt of the fatty acid in the 1 position is reacted with epichlorohydrin. The epoxy ester which is formed is then reacted with the free fatty acid in the 3 position to give the 1,3-diacylglycerols. Since this reaction induces considerable amounts of 1,2-diacylglycerols to form, the solid mixture is heated for a certain time at a temperature just below the melting point, which causes an isomerization of the fatty acid residue from the 2 to the 3 position. Finally, the 1,3-diacylglycerols are treated with the acid chloride of the fatty acid at the 2 position. When the fatty acid in the 2 position is very labile, the coupling can also be achieved with dicyclohexylcarbodiimide, which was used to stabilize the esterification reactions described here. The isomerization of 1,2-diacylglycerols to 1,3-diacylglycerols is only effective with solid esters at a sufficiently high melting point (e.g., between 50 and 60°C). At lower temperatures the isomerization is slow. So, in the case of SLS, epichlorohydrin was boiled with

*To whom correspondence should be addressed.
E-mail: kyosato@hiroshima-u.ac.jp

sodium stearate to yield the glycidyl stearate. This was heated with stearic acid, and the mixture of 1,2- and 1,3-diacylglycerols was heated at 55°C for several days until the isomerization was complete. Finally, the 1,3-distearate was treated with linoleic acid chloride and the TAG purified by crystallization. The purity of the product was at least 95%.

Differential scanning calorimetry (DSC). A Rigaku Thermoplus DSC 8230 instrument (Tokyo, Japan) was used for thermal measurements of polymorphic crystallization and transformation. The experiments were performed by using the following thermal treatments. For cooling processes, the sample was first kept at 60°C for 10 min, then cooled to –20°C at rates of 5, 15, and 20°C/min. For the heating process, the sample was kept at 60°C for 10 min, then cooled to –20°C at the rate of 20°C/min, held at –20°C for 10 min, and then heated to 60°C at the rates of 2 and 10°C. The temperatures of crystallization and transformation were defined by computerized data-processing as the crossing points of cooling or heating base lines and the maximal slopes of initial exothermic of endothermic lines (onset temperature).

X-ray diffraction (XRD). As for laboratory-scale XRD, powder XRD patterns were examined by a Nickel-filtered Cu-Kα radiation (λ = 0.1542 nm) to obtain short- and long-spacing values (Geigerflex, Rigaku). Synchrotron radiation XRD (SR-XRD) experiments were carried out at the National Laboratory for High Energy Physics (Tsukuba, Japan) by using a beam line BL-15A of the source which was operated at 2.5 GeV. The double-focusing camera was operated at a wavelength of 0.15 nm for the SR-XRD. Details of the equipment cell employed in the SR-XRD study have been described elsewhere (3,8). In brief, the X-ray scattering data were detected by position-sensitive proportional counters for the small angle position. The sample was placed in the center of a stainless steel sample cell with kapton film windows, which was sandwiched in a brass jacket. A quick temperature jump was performed by utilizing two thermostated water baths connected by a magnetic switch. The thickness of the sample was 1 mm, and the SR-XRD spectra were taken at 10-s intervals.

Fourier transform infrared spectroscopy (FTIR). The powder sample was compressed between two KBr windows, then melted at 60°C, and cooled to crystallize at various temperatures. IR spectra were collected using a PerkinElmer FTIR spectrometer (Spectrum 2000; Norwalk, CT), equipped with an i-series FTIR microscope.

RESULTS

Occurrence of polymorphic forms. The occurrence of polymorphic modifications was examined by two modes of crystallization. The first one was a simple cooling of liquid from 60°C to various temperatures of crystallization (T_c). The second crystallization was made by a melt-mediated transformation, in which more stable forms were crystallized after melting less stable forms by rapidly raising the temperature above their melting points.

Figure 1 shows the DSC cooling and heating thermopeaks of SLS at different rates of temperature variation. In Figure 1A, a single exothermic peak, at 24.3°C, appeared at a cooling rate of 5°C/min. However, additional peaks appeared around 11 and –2°C with increasing rates of cooling up to 20°C/min, while the thermopeak of 24.3°C at 5°C/min decreased to 21.6°C at 20°C/min. As fully explained later by employing the SR-XRD data, the exothermic peaks were assigned the transformations from liquid to α, from α to sub-α_1, and sub-α_1 to sub-α_2.

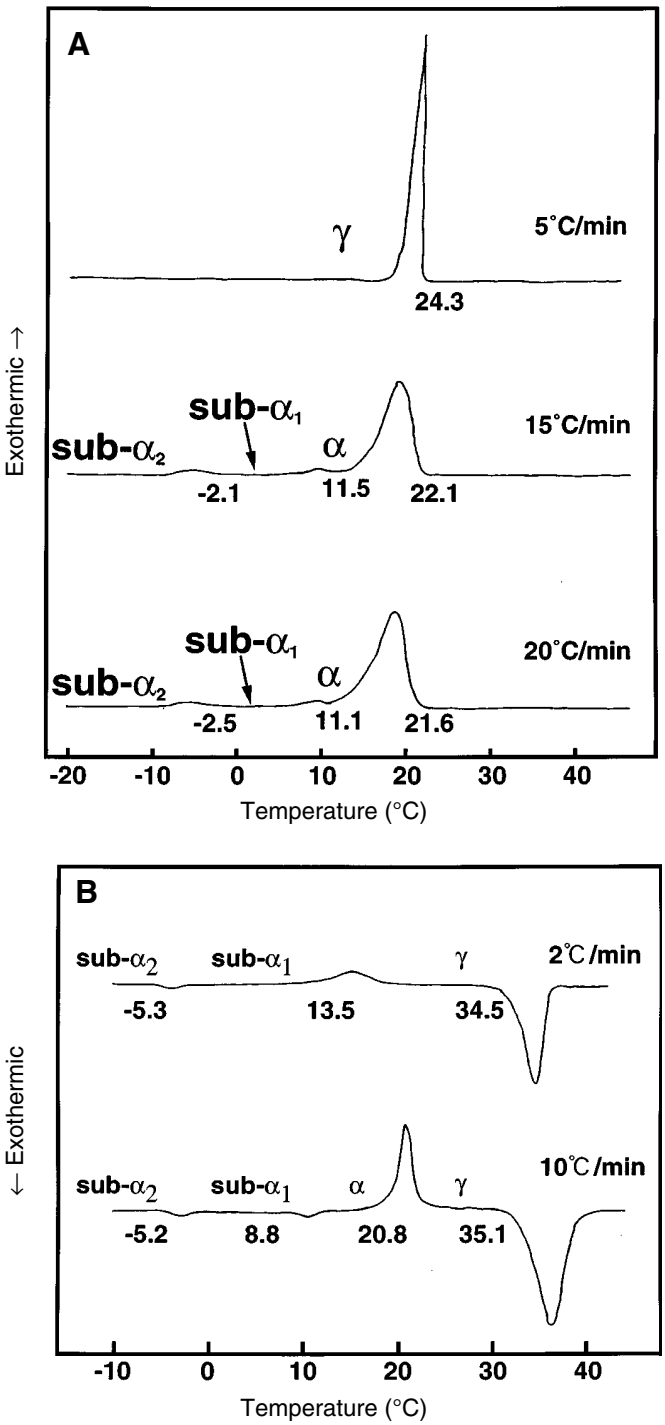

FIG. 1. Differential scanning calorimetry thermograms of 1,3-distearoyl-*sn*-2-linoleoyl-glycerol (SLS) at different rates of cooling (A) and heating (B).

Figure 1B shows the DSC thermopeaks observed during the heating process, which was carried out from –10 to 42°C soon after the crystallization from liquid at –10°C. At the heating rate of 2°C/min, two endothermic peaks at –5.3 and 34.5°C and an exothermic peak at 13.5°C were observed. With increasing rate of heating, additional peaks, one endothermic at 8.8°C, and the other exothermic at 20.8°C, were detectable. Similarly to Figure 1A, the SR-XRD data clarified that the endothermic peaks at –5.2 and 8.8°C correspond to the polymorphic transformations from sub-α_2 to sub-α_1, and from sub-α_1 to α, respectively, and that the melting of γ occurred at 35.1°C. The exothermic peak at 20.8°C was due to the transformation from α to γ. As for the result observed at 2°C/min, the transformations from sub-α_1 to γ through a occurred simultaneously, and thus the DSC endothermic and exothermic peaks were smeared out.

Figure 2 shows the XRD short-spacing spectra of γ, α, sub-α_1, and sub-α_2 forms. Table 1 summarizes the intensity ratios of the diffraction spectra, all of which were taken at temperatures indicated in Figure 2. The γ form showed almost the same XRD pattern as that for SOS and POP (2). The same was also true for the α form, which has single peak at 0.412 nm. As for the two sub-α forms, two diffraction peaks were observed for both, yet the values of sub-α_1 were slightly larger than those of sub-α_2. The differentiation of the two sub-α forms was clearly evidenced by temperature variation in the XRD spectra taken for the SLS sample, obtained by chilling the liquid to –20°C, and fluctuated around 5 and –20°C, as shown in Figure 3. This transformation between the two sub-α forms corresponded well to the DSC exothermic (cooling) and endothermic (heating) peaks shown in Figures 1A and 1B, respectively.

TABLE 1
Intensity Ratio of X-Ray Diffraction Short-Spacing Spectra of Polymorphic Forms of SLS[a]

Form	Short spacing (nm)				
Sub-α_2	0.419 (s)	0.374 (m)			
Sub-α_1	0.421 (s)	0.385 (m)			
α	0.412 (s)				
γ	0.381 (vs)	0.474 (s)	0.450 (m)	0.360 (m)	0.425 (w)

[a]s = strong, m = medium, w = weak; SLS, 1,3-distearoyl-*sn*-2-linoleoyl-glycerol.

Time-resolved synchrotron radiation (SR) XRD. Since the occurrence and subsequent transformations of SLS polymorphs were highly dependent on the rate of temperature variation, precise measurement of the polymorphic transformation was carried out in time-resolved and *in-situ* fashion. An SR X-ray beam was used for the rapid temperature variation, and laboratory-scale rotator-anode XRD was applied to the slow temperature variation.

Figure 4 shows the SR-XRD spectra taken under the tem-

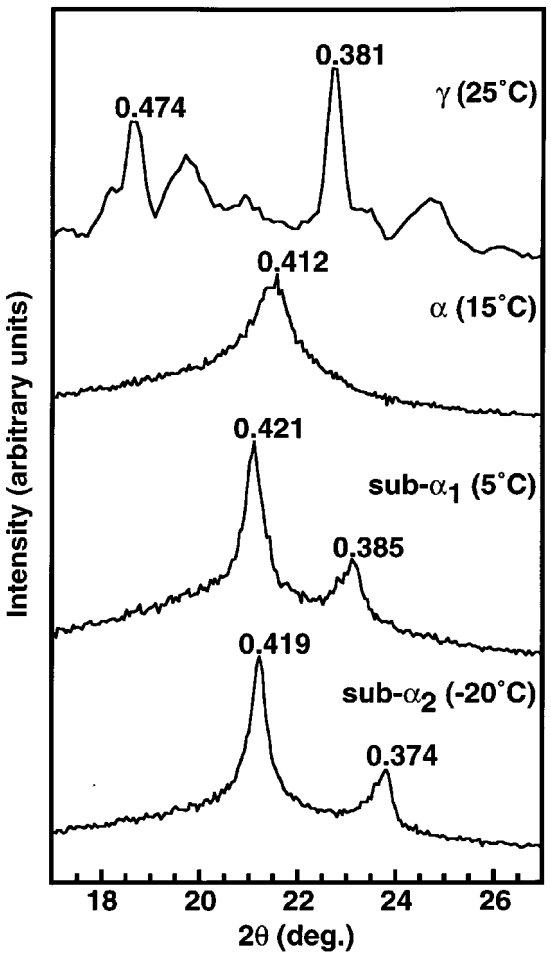

FIG. 2. X-ray diffraction short-spacing spectra of polymorphic forms of SLS (unit: nm). For abbreviation see Figure 1.

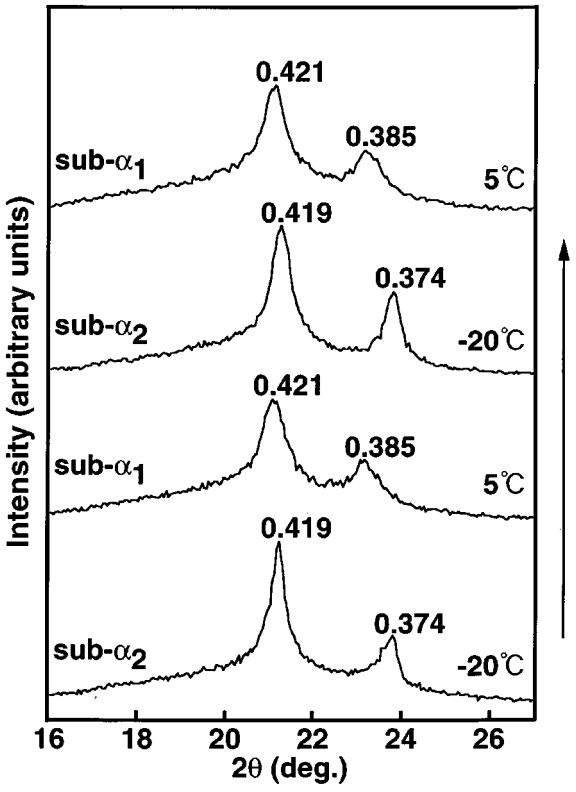

FIG. 3. *In-situ* X-ray diffraction spectra of reversible transformation from sub-α_2 to sub-α_1 (unit: nm).

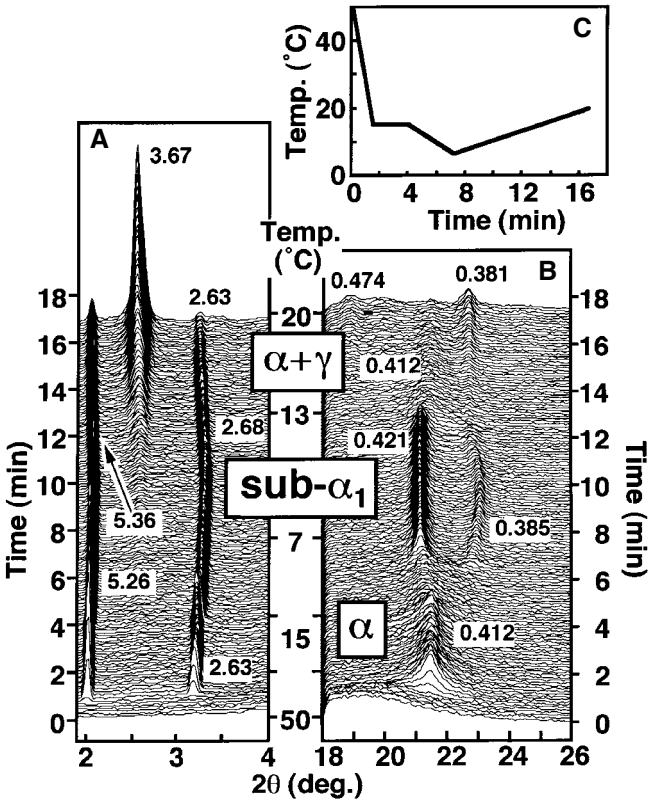

FIG. 4. Time-resolved synchrotron radiation X-ray diffraction spectra of transformations from α to sub-α_1, and from sub-α_1 to α + γ. (Temperature variation profile is inserted.) (unit: nm).

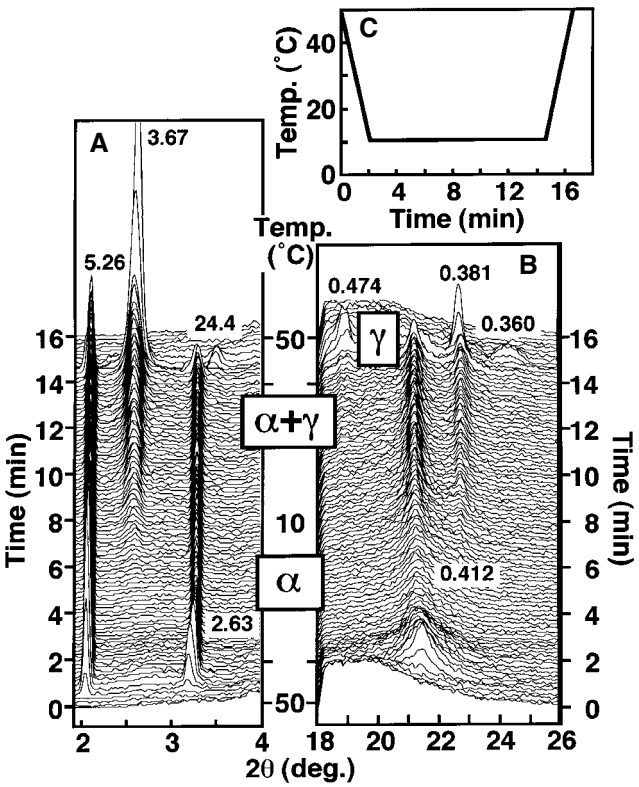

FIG. 5. Time-resolved synchrotron radiation X-ray diffraction spectra of transformation from α to γ. (Temperature variation profile is inserted.) (unit: nm).

perature variation in which a stepwise decrease was applied from 50 to 7°C through 15°C. This procedure enabled us to crystallize the α form, and to let the α form transform to sub-α_1 below 11°C. The subsequent heating from 7 to 15°C induced the transformation from sub-α_1 to both the α and γ forms. At 15°C after the chilling, the single spectrum of short spacing of α (0.412 nm) occurred together with long-spacing spectra of 5.26 (001) and 2.63 nm (002). On further cooling, the short-spacing spectrum of a disappeared, and two spectra of sub-α_1 appeared at 8°C. Correspondingly, long-spacing spectra shifted toward wider-angle regions, providing the value of 5.36 (001) and 2.68 nm (002), which are of the sub-α_1 form. The transformation from sub-α_1 to the high-temperature forms was observed, yet the short- and long-spacing spectra showed the simultaneous occurrence of the α and γ forms. In particular, the long-spacing spectrum of 3.67 nm was already evident at around 10°C, as indicated at a time of 10 min, measured from the beginning of the temperature variation. However, the conversion from sub-α_1 to α revealed in the long-spacing spectra was continuous, making a contrast to the conversion into the γ form. During the heating process from 15 (15 min) to 20°C (17 min), the long spacing spectrum of γ rapidly increased in intensity at the expense of those of the α form.

Figure 5 shows the occurrence of α and subsequent transformation into γ. The thermal treatment was the following: liquid was chilled from 50 to 10°C, kept at 10°C for about 10 min, and heated rapidly to 50°C. In this case, no sub-α_1 was observed since this form transformed to α at 8.8°C, as shown in Figure 1B. The rapid heating from 10 to 50°C clearly showed the transformation from α to γ at 20°C, which was detected by the rapid heating DSC thermopeak shown in Figure 1B, in which the exothermic peak at 20°C corresponded to this conversion. As also shown in Figure 5A, the γ form started to occur at 10°C at 8 min during the temperature variation.

The results of Figure 5 mean that the slow heating process resulted in the gradual conversion from α to γ, whereas the rapid heating induced the α-γ transformation with an exothermic heat of transformation. This property was clearly shown by the time-resolved XRD study using rotator-anode apparatus at the heating rate of 2°C/min, as shown in Figure 6. The sub-α_2 form, crystallized by chilling the liquid from 60 to –20°C, sequentially transformed to sub-α_1 and eventually to γ. No α form was detectable during this slow heating process, because the transformation into the most stable γ form occurred without the passage of the α form.

FTIR spectra. The FTIR spectra of sub-α_1, α, and γ were taken at temperatures of 5, 15, and 25°C, respectively, as shown in Figure 7. Attention was paid to the polymethylene rocking mode, r(CH_2) and the scissoring mode, δ(CH_2), both of which are sensitive to subcell packing of the TAG crystals (13), as summarized in Table 2. Doublet spectra were ob-

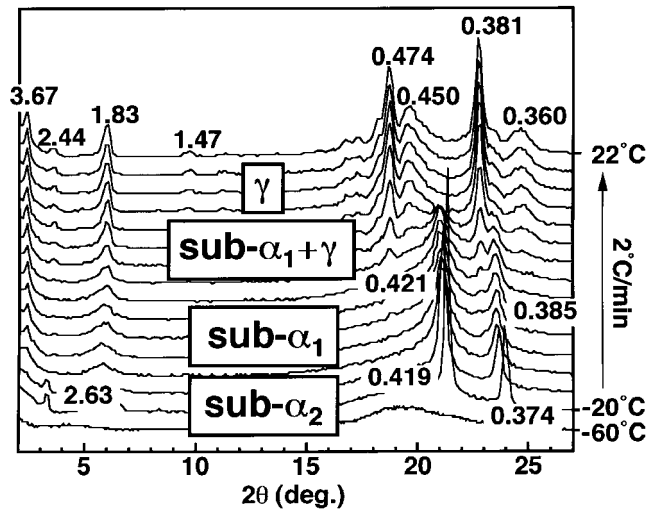

FIG. 6. *In-situ* rotator-anode X-ray diffraction spectra of transformation from sub-α_2 to γ (unit: nm).

served in r(CH_2) and δ(CH_2) for the sub-α_1 form, indicating pseudohexagonal packing, which was recently analyzed in detail for the sub-α form of SOS (14). By contrast, the α and γ forms showed single bands for the two vibration modes. The

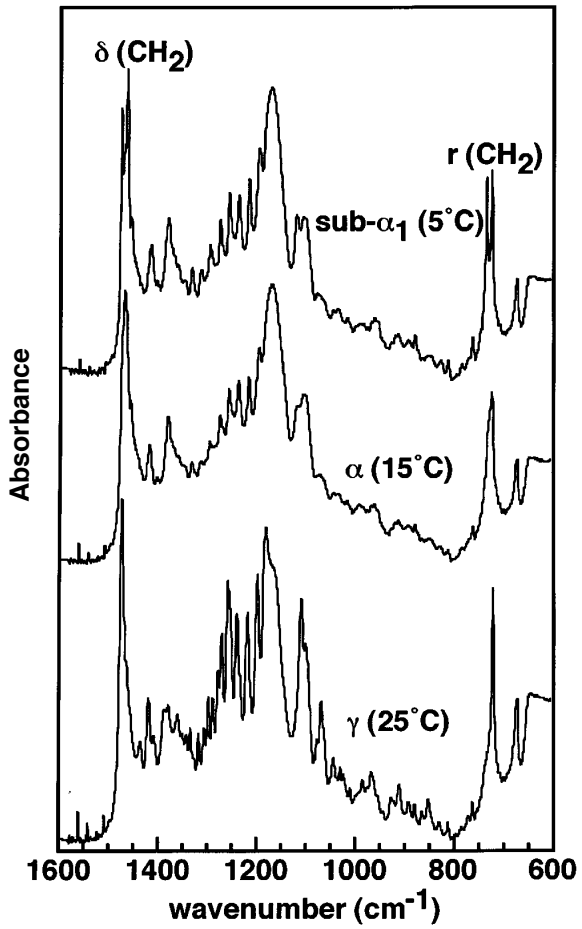

FIG. 7. Fourier transform infrared absorption spectra bands of polymorphic forms of SLS. For abbreviation see Figure 1.

TABLE 2
FT-IR Absorption Bands (cm^{-1}) of Polymorphic Forms of SLS[a]

	–CH_2 scissoring [γ(CH_2)]	–CH_2 rocking [r(CH_2)]
Sub-α_1	1474, 1466.5	731, 719
α	1467	719.5
γ	1471.5	717.5

[a]For abbreviation see Table 1.

wavenumber values of the two forms indicate the subcell packing of hexagonal for α and parallel type for γ (15).

DISCUSSION

The present study confirmed the presence of four polymorphs in SLS, whose thermodynamic parameters, chain length structure, and subcell structures were obtained by DSC, XRD, and FTIR experiments. The thermal data obtained are summarized in Tables 3 and 4 from the cooling and heating DSC thermopeaks, respectively. Table 5 shows the chain-length structure and subcell packing structures. The transformations from sub-α_2 to sub-α_1, and from sub-α_1 to α are associated with small values of enthalpy and entropy, indicating that the structural differences might not be remarkable, in compari-

TABLE 3
Thermal Properties of Polymorphic Transformations of SLS (for cooling processes)

	T (°C)	Δ*H* (kJ/mol)[a]	Δ*S* (J/mol/K)[a]
Melt ~ γ^b	24.3	139.5	469.0
Melt ~ α^c	21.6	66.0	223.8
α ~ sub-$\alpha_1{}^c$	11.1	NA[d]	NA[d]
Sub-α_1 ~ sub-$\alpha_2{}^c$	–2.5	2.6	9.7

[a]Δ*H*, enthalpy of transformation; Δ*S*, entropy of transformation.
[b]Cooling rate: 5°C/min.
[c]Cooling rate: 20°C/min.
[d]Not available. For other abbreviations see Table 1.

TABLE 4
Thermal Properties of Polymorphic Transformations of SLS (for heating processes)

	T (°C)	Δ*H* (kJ/mol)[a]	Δ*S* (J/mol/K)[a]
Sub-α_2 ~ sub-$\alpha_1{}^b$	–5.3	3.7	13.7
Sub-α_1 ~ α^c	8.8	4.2	14.9
α ~ γ^c	20.8	40.9	139.2
γ ~ melt^b	34.5	137.4	446.7

[a]Δ*H*, enthalpy of transformation; Δ*S*, entropy of transformation.
[b]Heating rate: 2°C/min.
[c]Heating rate: 10°C/min. For abbreviations see Table 3.

TABLE 5
Structural Properties of Polymorphic Forms of SLS[a]

	Chain-length structure	Subcell packing
Sub-α_2	2	Pseudo-H
Sub-α_1	2	Pseudo-H
α	2	H
γ	3	//-type

[a]For abbreviations see Table 1.

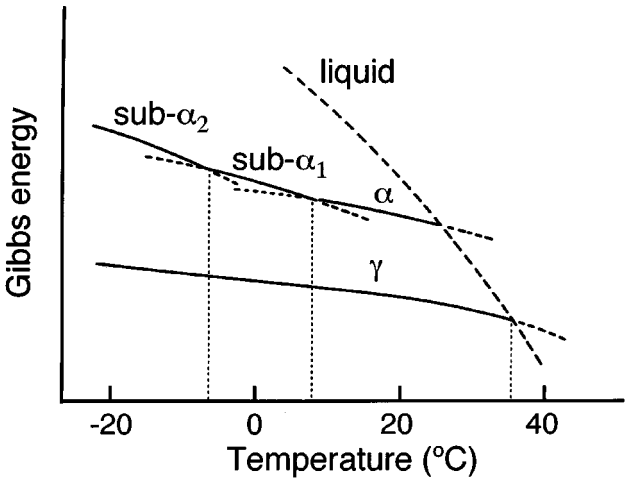

FIG. 8. A tentative relationship between Gibbs energy and temperature for four polymorphic forms of SLS. For abbreviation see Figure 1.

son to that from α to γ. The chain-length structures are double in the two sub-α forms and α, whereas γ was of the triple chain-length structure. The entropy value of melting of γ is larger than that of γ of SOS (319.2 J/mol/K) (2). This indicates more ordered structure in γ of SLS than γ of SOS, mostly because of the presence of the two *cis* double bonds in the linoleoyl moiety of SLS. The long spacing value of γ, 7.33 nm, was longer than γ of SOS (7.05 nm).

Figure 8 illustrates a tentative relationship between Gibbs energy (*G*) and temperature (*T*) for the four polymorphs and liquid. The reversible transformation between sub-α_1 and sub-α_2 and reversible transformation between sub-α_1 and α are shown in an enantiotropic relation, whereas the γ form is most stable at the all temperatures examined in the present study. As for the relationship between α and γ, the exothermic heat released during the solid state transformation indicates that the two forms may not be related by the enantiotropic relation, as shown in Figure 8. This means the presence of a unique melting point of α, as revealed for α of SOS. However, the melting point of α of SLS was not detectable in the present study, even under rapid heating in the DSC experiment. This indicates that the α form of SLS is a metastable form which quite easily transforms to γ. The reason for this rapid α–γ transformation may be ascribed to more preferred structure of γ of SLS whose stability is enabled by the cooperative interactions of the two *cis*-double bonds of the linoleic acid chains. It follows that the chain-chain interactions between the linoleic acid moieties eventually make γ the most stable polymorph of SLS.

Scheme 1 illustrates structural models of sub-α, α, and γ of SLS, in which the differentiation between the two sub-α forms is not made. The sub-α and α forms are stacked in the double chain-length structure in which the stearoyl and linoleoyl chain are packed in the same leaflet. Since the steric hindrance between the stearoyl and linoleoyl chains is limiting, chain segregation occurs during the α–γ transformation. This results in the formation of the triple chain-length γ form, in which the stearoyl and linoleoyl chains are packed in different leaflets. It is speculated that the degree of steric hindrance between the stearoyl and linoleoyl chains in SLS is so intense that the α form is quite unstable and transforms into γ very easily, as observed in the DSC and XRD measurements.

The peculiarity in the polymorphic behavior of SLS, in comparison to SOS, is the absence of β′ and β forms, which are often observed in most of the St.-Oleic-St. TAG (14). The structural properties of the β′ and β forms of SOS are summarized in the following: (i) orthorhombic perpendicular subcell is present and aliphatic acid chains are inclined by about 72° in β′, and (ii) triclinic parallel subcell is formed and the

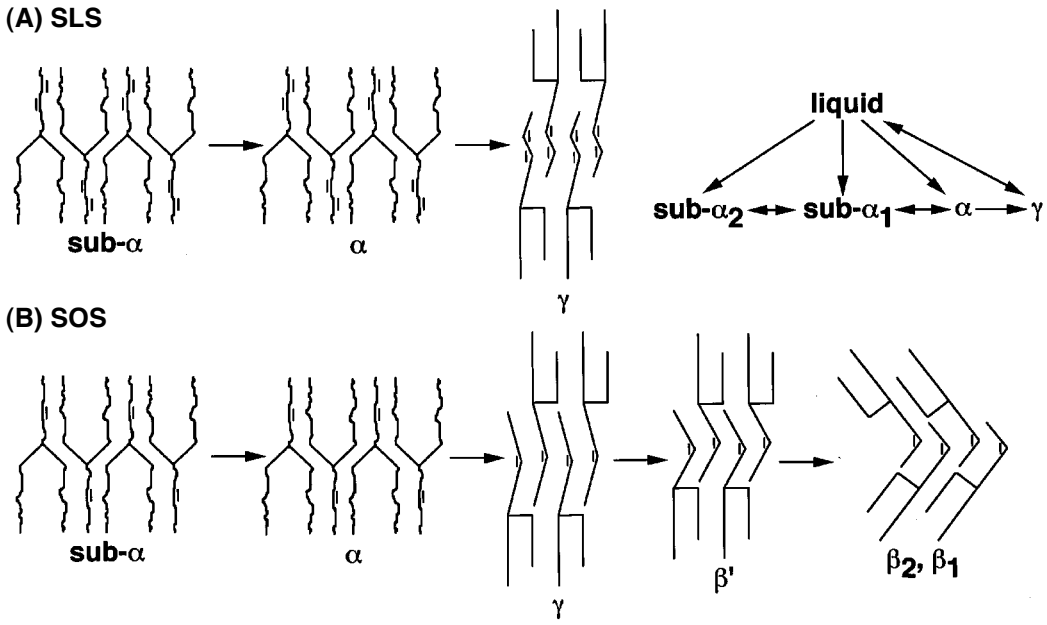

SCHEME 1

chains are inclined by about 52° in β. By contrast, the γ form in SOS contains a parallel-type subcell for the stearoyl chains, and non-specific subcell is formed in the oleoyl leaflet because of the rather disordered molecular conformation (2). Taking into account these structural properties of SOS, one may assume that the reason for the absence of the β′ and β forms in SLS may be the disordered molecular conformation of the linoleoyl chain. The flexible conformation of the linoleoyl chain may prohibit the transformation into the β′ and β form which require the stabilization of the subcell packing of the stearoyl chains for β′, in the first, and the linoleoyl chains in the most stable form of β, as revealed in SOS (14). This situation is somewhat similar to the polymorphism of SRS (8), in which hydrogen bonding in the ricinoleoyl chains in β′ does not allow the transformation into β, and thereby the most stable form of SRS is β′.

REFERENCES

1. Gurr, M.I., Lipids and Nutrition, in *Lipid Technologies and Applications,* edited by F.D. Gunstone and F.B. Padley, Marcel Dekker, Inc., New York, 1997, pp. 79–112.
2. Sato, K., T. Arishima, Z.H. Wang, K. Ojima, N. Sagi, and H. Mori, Polymorphism of POP and SOS. I. Occurrence and Polymorphic Transformation, *J. Am. Oil Chem. Soc. 66*:664–674 (1989).
3. Ueno, S., A. Minato, H. Seto, Y. Amemiya, and K. Sato, Synchrotron Radiation X-ray Diffraction Study of Liquid Crystal Formation and Polymorphic Crystallization of SOS (*sn*-1,3-distearoyl-2-oleoyl-glycerol), *J. Phys. Chem. 101*:6847–6854 (1997).
4. Yano, J., S. Ueno, K. Sato, T. Arishima, N. Sagi, F. Kaneko, and M. Kobayashi, FT-IR Study of Polymorphic Transformations in SOS, POP, and POS, *J. Phys. Chem. 97*:12967–12973 (1993).
5. Arishima, T., N. Sagi, H. Mori, and K. Sato, Polymorphism of POS. I. Occurrence and Polymorphic Transformation, *J. Am. Oil Chem. Soc. 68*:710–715 (1991).
6. Hachiya, I., T. Koyano, and K. Sato, Seeding Effects on Solidification Behavior of Cocoa Butter and Dark Chocolate. I. Kinetics of Solidification, *Ibid. 66*:1757–1762 (1989).
7. Lavery, H., Differential Thermal Anaysis of Fats. II. Melting Behavior of Some Pure Glycerides, *Ibid. 35*:418–422 (1958).
8. Boubekri, K., J. Yano, S. Ueno, and K. Sato, Polymorphic Transformations *in* sn-1,3-Distearoyl-2-ricinoleyl-glycerol, *Ibid. 76*: 949–955 (1999).
9. Chapkin, R.S., Reappraisal of the Essential Fatty Acids, in *Fatty Acids in Foods and Their Health Implications,* edited by C.K. Chow, Marcel Dekker, Inc., New York, 1992, pp. 429–436.
10. List, G.R., T.L. Mounts, F. Orthoefer, and W.E. Neff., Effect of Interesterification on the Structure and Physical Properties of High-Stearic Acid Soybean Oils, *J. Am. Oil Chem. Soc. 74*: 327–329 (1997).
11. List, G.R., T.L. Mounts, F. Orthoefer, and W.E. Neff, Potential Margarine Oils from Genetically Modified Soybeans, *Ibid. 73*: 729–732 (1996).
12. Mank, A.P.J., J.P. Ward, and D.A. van Drop, A Versatile, Flexible Synthesis of 1,3-Diglycerides and Triglycerides, *Chem. Phys. Lipids. 16*:107–114 (1976).
13. Kobayashi, M., Vibrational Spectroscopic Aspects of Polymorphism and Phase Transition of Fats and Fatty Acids, in *Crystallization and Polymorphism of Fats and Fatty Acids,* edited by N. Garti and K. Sato, Marcel Dekker, Inc., New York, 1988, pp. 139–187.
14. Yano, J., K. Sato, F. Kaneko, D.M. Small, and D.R. Kodali, Structural Analyses of Polymorphic Transitions of *sn*-1,3-Distearoyl-2-oleoylglycerol (SOS)and *sn*-1,3-dioleoyl-2-stearylglycerol (OSO): Assessment of Steric Hindrance of Unsaturated and Saturated Acyl Chain Interactions, *J. Lipid Res. 40*: 140–151 (1999).
15. Hernqvist, L., Crystal Structures of Fats and Fatty Acids, in *Crystallization and Polymorphism of Fats and Fatty Acids,* edited by N. Garti and K. Sato, Marcel Dekker, Inc., New York,

1988, pp. 97–137.

[Received February 29, 2000; accepted August 19, 2000]